Separation Science and Technology
Publication details, including instructions for authors and subscription information:
http://www.informaworld.com/smpp/title~content=t713708471

Modeling chromatographic purification of rh-bFGF with Heparin HyperD affinity sorbent using a homogeneous and a pore diffusion model

Gunnar Garke[a]; Wolf-Dieter Deckwer[b]; Friedrich Birger Anspach[c]
[a] Biochemical Engineering Division, Mascheroder Weg 1, IBA Biologics GmbH, Braunschweig, Germany [b] Biochemical Engineering Division, Mascheroder Weg 1, GBF-Gesellschaft für Biotechnologische Forschung, Braunschweig, Germany [c] PHARIS Biotec GmbH, Hannover, Germany

Online publication date: 29 May 2002

SEPARATION SCIENCE AND TECHNOLOGY, 37(7), 1521–1544 (2002)

MODELING CHROMATOGRAPHIC PURIFICATION OF rh-bFGF WITH HEPARIN HyperD AFFINITY SORBENT USING A HOMOGENEOUS AND A PORE DIFFUSION MODEL

Gunnar Garke,[1] Wolf-Dieter Deckwer,[2] and Friedrich Birger Anspach[2,*]

[1]IBA Biologics GmbH and
[2]GBF-Gesellschaft für Biotechnologische Forschung,
Biochemical Engineering Division, Mascheroder Weg 1,
38124 Braunschweig, Germany

ABSTRACT

On the basis of the purification of recombinant human basic fibroblast growth factor (rh-bFGF), the prediction of exact protein adsorption and gradient elution by two mathematical models was investigated. To this end, thermodynamic and kinetic parameters were employed from batch experiments. These were evaluated from both the film and pore diffusion (FPD) and the homogeneous diffusion model, and applied to a packed bed. The adsorption of rh-bFGF as a function of the salt concentration on Heparin HyperD was well described by the Langmuir model. It was possible to adopt the functional connection between ionic strength

*Corresponding author. Current address: PHARIS Biotec GmbH, Karl-Wiechert-Allee 76, 30625 Hannover, Germany. E-mail: FBAnspach@aol.com

and dissociation constant as well as maximal adsorption capacity for the calculation of elution processes using the FPD model. Uptake curves displayed a significant increase in the effective pore diffusion coefficient, D_p, with decreasing protein concentration, which is indicative for surface diffusion. In contrast, the coefficient for homogeneous diffusion, D_h, was independent of the protein concentration. Adaptation to the packed bed required a substantial increase in both D_p and D_h. Although this could be seen as an indication of convective flow in the sorbent, data from different and relatively slow mobile phase velocities clearly indicated absence of intra particulate flow. For an exact prediction of the adsorption process over the wide range of concentrations applied here, a still deeper insight into protein adsorption and desorption is needed to discriminate among the various diffusion and adsorption phenomena.

INTRODUCTION

A broad application of model-supported procedures for the processing and optimization in preparative chromatographic purification of proteins today still faces a strongly pronounced modeling bottleneck regarding real applications. The reasons for this are complex physicochemical interactions of the innumerable components in mixtures of biological origin. Furthermore, the macromolecular characteristics of proteins likely produce additional problems (1), such as variations of surface charge densities with pH, conformational changes during adsorption, etc.

Mathematical models for preparative chromatography developed in recent years evolved from the similarity to thermal separation processes, such as rectification, extraction, and adsorption (2). In these processes, the nonequilibrium of the different phases is considered as driving force. Mass transport processes are restricted by the properties of the stationary and the mobile phases and so their analysis and description play a central role in these models. The bases are therefore equations for the preservation of masses. Generally, the adsorption is described as unsteady packed bed process, where moving fronts proceed through the column. Apart from several theoretical models and parameter studies (3–5), applications are described using model proteins [see Refs. (6–8) for example].

The following investigation was done in order to examine the suitability of the film and pore diffusion (FPD) model as well as the homogeneous diffusion model regarding their applicability in context of a "real" system. As an example, for the modeling of chromatographic processes, the affinity purification of recombinant human basic fibroblast growth factor (rh-bFGF) by means of a

heparin sorbent was selected. The rh-bFGF is a single-chain, nonglycosylated protein containing 154 amino acids with a molar mass of 17.3 kDa. It modulates both cell proliferation and differentiation in vitro and in vivo (9). The affinity purification of this protein represents the second of a two-stage purification procedure starting from an *Escherichia coli* high cell-density cultivation (10). The first stage, after cell disruption, consists of an expanded bed adsorption process using a cation exchanger (11). Most important for the modeling of the affinity chromatographic step was the mathematical simulation of the gradient elution. In order to apply the model for process description or optimization, it is further envisaged that the modification of process parameters, such as the flow rate, can be depicted without further adjustments of model parameters.

THEORETICAL CONSIDERATIONS

For modeling, the FPD model as well as the homogeneous diffusion model was applied, on the basis of the well-known differential mass balance equations (2). Hence the column is divided into a mobile and a stationary phase.

The mass transfer equation of the mobile phase considers accumulation, convective, and diffusive flow along the z-direction as well as mass transfer to the particular stationary phase:

$$\varepsilon_b \frac{\partial c_{b,i}}{\partial t} = \varepsilon_b D_{ax} \frac{\partial^2 c_{b,i}}{\partial z^2} - \varepsilon_b u_i \frac{\partial c_{b,i}}{\partial z} - \frac{3}{R_p}(1 - \varepsilon_b) k_{f,i}(c_{b,i} - c_{p,i|R=R_p}) \qquad (1)$$

with $c_{b,i}$ and $c_{p,i}$ are the concentrations of component i in the bulk phase and the pore liquid at the particle edge, respectively, ε_b the bulk porosity, D_{ax} the axial dispersion coefficient, u_i the interstitial velocity, R_p the particle radius, and k_f the film mass transfer coefficient.

Film and Pore Diffusion Model

In the FPD model, the stationary phase is subdivided into the solid phase $(1 - \varepsilon_p)$ and the pore liquid (ε_p), whereby the mass transport takes place only in the pore volume according to the principle of free diffusion. Considering the amount of solute reduced by adsorption, the mass balance for the pore liquid along the radius of the sorbent particle, r, is obtained:

$$\varepsilon_{p,i} \frac{\partial c_{p,i}}{\partial t} = \varepsilon_{p,i} D_{p,i} r^{-2} \frac{\partial}{\partial r}\left[r^2 \frac{\partial c_{p,i}}{\partial r}\right] - (1 - \varepsilon_{p,i}) \frac{\partial q_i}{\partial t} \qquad (2)$$

The pore diffusion coefficient, $D_{p,i}$, is derived from the diffusion coefficient in solution, $D_{b,i}$, considering pore fraction and tortuosity

$$D_{p,i} = \frac{D_{b,i}\varepsilon_{p,i}}{\tau} \tag{3}$$

Typically, τ adopts values between 2 and 6 (2,12). The mass loss in the mobile phase due to adsorption in the model is considered using:

$$\frac{\partial q_i}{\partial t} = k_{a,i}c_{p,i}(q_{m,i} - q_i) - k_{d,i}q_i \tag{4}$$

Due to the large amount of negative charges on the heparin ligand, fast adsorption kinetics can be assumed, similar to cation exchange adsorbers. Therefore, it is reasonable to assume $\partial q/\partial t = 0$, which also was not contradicted by the experiments. Then Eq. (4) reduces to the Langmuir equation with saturation capacity, q_m, and dissociation constant $K_D = k_d/k_a$, which was employed in the modeling.

$$q_i^* = \frac{q_m c_{p,i}^*}{c_{p,i}^* + K_{D,i}} \tag{5}$$

Correspondingly, for mathematic modeling of a column system, a set of three differential equations [Eqs. (1), (2) and (4)] is obtained, which can be solved numerically by considering the following initial and boundary conditions.

$$t = 0: \quad c_{b,i} = c_{b,i}(0,z); \quad c_{p,i} = c_{p,i}(0,r,z); \quad q_i = q_i(0,r) \tag{6}$$

$$z = 0: \quad D_{ax}\frac{\partial c_{b,i}}{\partial z} = u_i(c_{b,i} - c_{0,i}(t)); \quad z = L: \quad \frac{\partial c_{b,i}}{\partial z} = 0 \tag{7}$$

$$r = 0: \quad \frac{\partial c_{p,i}}{\partial r} = 0; \quad r = R_p: \quad D_{p,i}\varepsilon_{p,i}\frac{\partial c_{p,i}}{\partial r} = k_{f,i}(c_{b,i} - c_{p,i|r=R_p}) \tag{8}$$

After transformation to the dimensionless form, these equations were integrated with the aid of FORTRAN library functions. A description of the detailed procedure as well as a program listing is described elsewhere (13).

The salt used for gradient elution was implemented as a second component within the model using a diffusion coefficient of sodium chloride of $D_p = 1.84 \times 10^{-10}\,m^2\,sec^{-1}$. The second set of differential equation for the salt was solved simultaneously with the protein, so the Langmuir parameter could be calculated.

Homogeneous Diffusion Model

With regard to the homogeneous diffusion model, the stationary phase is assumed as a homogeneous phase in which diffusion takes places. Thus, the structure of the stationary phase is not considered explicitly but implicitly in the homogeneous diffusivity:

$$\frac{\partial q_i}{\partial t} = D_{\mathrm{h},i} r^{-2} \frac{\partial}{\partial r}\left[r^2 \frac{\partial q_i}{\partial r}\right] \tag{9}$$

With this model, the adsorption isotherm is only considered at the edge of the adsorbent particle. The concentration at the edge of the particle, c_s, is coupled with the concentration in the mobile phase, c_b, via the film mass transfer coefficient, k_f. Considering the Langmuir adsorption isotherm at $r = R_\mathrm{p}$, a modified boundary condition follows compared to the pore diffusion model [see Eq. (8)].

$$\begin{aligned} r = 0: \quad & \frac{\partial q_i}{\partial r} = 0; \\ r = R_\mathrm{p}: \quad & D_{\mathrm{h},i} \frac{\partial q_i}{\partial r} = k_{\mathrm{f},i}(c_{\mathrm{b},i} - c_{\mathrm{s},i}(q_i^*)_{|r=R_p}) \\ & = k_{\mathrm{f},i}\left(c_{\mathrm{b},i} - \frac{q_i^* K_{\mathrm{D},i}}{q_{\mathrm{m},i} - q_i^*}\right) \end{aligned} \tag{10}$$

Axial Dispersion and Film Transport

For the modeling of the column experiments both the axial dispersion and the film mass transfer coefficients were expressed by correlations from literature. Residence time distribution studies with acetone (data not shown) demonstrated that the axial dispersion was well described by the correlation of Chung and Wen (14) within the examined flow rates, up to 534 cm hr^{-1}.

$$Pe_0 = 0.20 + 0.011 Re_0^{0.48} \tag{11}$$

The film mass transfer coefficient was estimated according to the empirical correlation from Wilson and Geankoplis (15). This correlation considers fluid (Re) and material properties (Sc) of the medium. It is valid for Re numbers between $0.0016 < Re < 55$ and porosities between $0.35 < \varepsilon_\mathrm{b} < 0.75$.

$$k_\mathrm{f} = \frac{D_\mathrm{b}}{d_\mathrm{p}} \frac{1.09}{\varepsilon_\mathrm{b}} (Re_0 Sc)^{0.33} \tag{12}$$

Batch Uptake Model

Modeling of uptake curves in stirred tank experiments was performed according to the employed model with mass balance equations of the stationary phase as in the column model Eq. (2) or (9). The concentration, or rather the mass, in the interparticulate fluid phase (batch phase, ε_b) results from the introduced mass at the beginning (c^0, $t = 0$), neglecting the mass in the pore volume of the particles, by integration over the particle radius r.

$$c_b(t) = c^0 - \frac{(1 - \varepsilon_p)}{\varepsilon_b} \frac{3(1 - \varepsilon_b)}{R_p^3} \int_0^{R_p} q(r) r^2 \mathrm{d}r \tag{13}$$

EXPERIMENTAL

Materials

Ethylenediaminetetraacetic acid disodium salt dihydrate (EDTA) was obtained from Fluka (Buchs, Switzerland). Other chemicals and salts were purchased from E. Merck (Darmstadt, Germany) in analytical grade.

For the affinity chromatography studies the Heparin HyperD support with 70 μm (Lot: 5121) from BioSepra (Villeneuve la Garenne, Cedex, France) was employed. Before use, it was equilibrated with buffer and salt corresponding to the conditions employed in the experiments.

Recombinant human basic fibroblast growth factor was produced in a high cell density cultivation of *E. coli* TG1:pλFGFB as described (10). After cell harvest and cell disruption, the protein was prepurified by expanded bed chromatography (11).

Adsorption Isotherms

Determination of adsorption isotherms was carried out in small batch experiments using purified rh-bFGF. Plastic test tubes (Nunc GmbH, Wiesbaden, Germany) were used, which were slowly rotated after transferring the Heparin HyperD sorbent and the solution of known mass and protein concentration into the test tubes to achieve equilibrium (after 4 hr) at 20°C. The sorbent was equilibrated beforehand with the respective buffer; also the rh-bFGF solution was dialyzed accordingly. The adsorbed mass, q^*, of the sorbent was calculated from the mass difference between introduced amount of rh-bFGF and the amount in solution at equilibrium, c^*, by means of a UV detector set to 280 nm.

Protein Uptake Curves

For the measurement of the adsorption kinetics with purified rh-bFGF solutions a stirred ultrafiltration cell was used as reactor (Millipore GmbH, Eschborn, Germany). The cell was stirred at a constant rate of 400 rpm. The concentration of rh-bFGF was monitored continuously through recirculation by means of a peristaltic pump (Microperpex 2132, LKB, Bromma, Sweden) through a photometer (Uvicord SII, Pharmacia LKB, Sweden) with the wavelength set to 280 nm. The Heparin HyperD sorbent was retained by a flat sheet microfiltration membrane of cellulose acetate (Sartorius GmbH, Göttingen, No. 11106 47 N) with a nominal pore size of 0.45 μm.

Packed Bed Experiments

The Heparin HyperD sorbent was packed in a column HR 10/10 (Pharmacia Biotech, Uppsala, Sweden), according to the instructions of the manufacturer. The resulting dimensions of the packed bed were 10.8 × 1 cm with a bed volume of 8.5 mL. The column was used in conjunction with standard FPLC equipment (FPLC 500, Pharmacia Biotech, Uppsala, Sweden) and a UV detector (UV 2510 UVICORD SD, LKB, Bromma, Sweden) set to 278 nm.

Before application of rh-bFGF, the column was rinsed with 10 column volumes (CV) buffer A, consisting of 50 m*M* sodium phosphate (NaPi) + 1 m*M* EDTA + the indicated quantity of NaCl (pH 6.3). Flow rates were set between 153 and 458 cm hr^{-1}. After loading up to 90 mL sample volume containing rh-bFGF, 3 CV buffer A were used for washing following gradient elution with 26 CV up to 3 *M* NaCl in buffer A.

Determination of Volume Fractions of the Column

The void volume fraction, ε_b, and the pore volume fraction of stationary phase, ε_p, were determined under nonbinding conditions at 1.5 *M* NaCl in the packed bed mode. With dextran blue 2000 $\varepsilon_b = 0.466$ was determined. Lysozyme (14.4 kDa) was employed instead of bFGF (17.3 kDa) as the latter still demonstrated interactions at this high ionic strength; an ε_p of 0.662 was measured.

Numerical Simulations

Differential equations were solved using FORTRAN programs and applying the NAG (16) libraries D03 (Numerical Algorithm Group, Oxford, UK).

Compiled programs were executed on a SGI PowerChallenge (Silicon Graphics Inc., California).

RESULTS AND DISCUSSION

Adsorption Isotherms

To calculate the peak position during elution with salt gradients, protein adsorption isotherms on the heparin sorbent as a function of the salt concentration must be known. The adsorption behavior of rh-bFGF on Heparin HyperD, as deduced from batch experiments, can be fitted to the Langmuir Eq. (11). The apparent thermodynamic parameters q_m and K_D are both dependent on the ionic strength at salt concentrations between 0 and 1.4 *M* NaCl.

Both the maximal protein capacity, q_m, and the dissociation constant, K_D, can be expressed by means of simple relations as function of the salt concentration and can be integrated within the model for the packed column. As shown in Fig. 1, the saturation capacity for rh-bFGF on Heparin HyperD is quite high with $q_m = 150\,\mathrm{mg\,mL^{-1}}$ at 0 *M* NaCl and decreases linearly with increasing salt concentration. Extrapolation of these measurements would yield $q_m = 0\,\mathrm{mg\,mL^{-1}}$ at a salt concentration of about 1.6 *M* NaCl, i.e., no adsorption sites are available anymore. Although this is an oversimplification—always some protein retention will take place due to weak hydrophobic interactions—Fig. 1 indicates that the linear dependency does not deviate even at high salt concentration (1.4 *M* NaCl).

The course of the dissociation constant K_D as function of the salt concentration can be described by an exponential curve-fitting algorithm. The interaction of the present affinity system is driven mainly by electrostatic interactions of four closely neighbored lysine and one arginine residue at bFGF and the corresponding negative charges at the polyanion heparin (bFGF–heparin complex, Brookhaven data bank code: 2FGF; 17). Therefore, this affinity interaction is reduced with increasing salt concentrations.

Batch Uptake Curves

For the determination of the effective mass transport coefficient of rh-bFGF into the particles, parameters of the FPD model were estimated by fitting with the experimental data. Figure 2 shows uptake curves with different initial concentrations. It was necessary to increase the pore diffusion coefficient, D_p, from 2.5×10^{-12} to $9.5 \times 10^{-12}\,\mathrm{m^2\,sec^{-1}}$ with decreasing the concentration of rh-bFGF from $c^0 = 2.25\,\mathrm{mg\,mL^{-1}}$ at the beginning to $c^0 = 0.28\,\mathrm{mg\,mL^{-1}}$

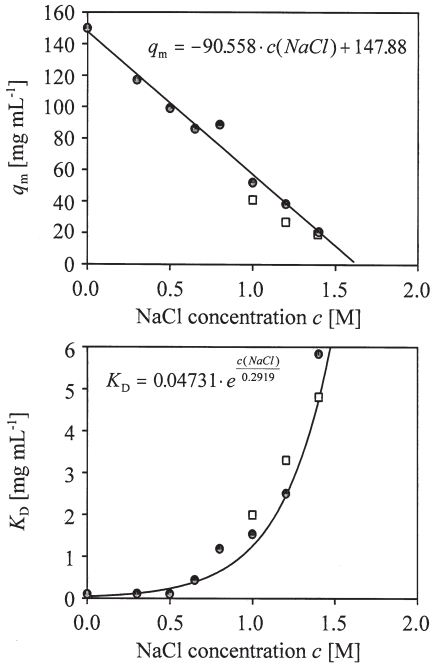

Figure 1. Dependency of the Langmuir parameters q_m (top) and K_D (bottom) on the salt concentration of rh-bFGF adsorption on Heparin HyperD in 50 m*M* sodium phosphate + 1 m*M* EDTA+NaCl, pH 6.3; (●) from batch adsorption isotherms, (□) adjusted values from isocratic elution.

(Table 1). As the FPD model relies on a concentration-independent pore diffusion coefficient, this behavior cannot be explained conclusively; the boundary condition is violated. It requires that in the model a concentration dependency of D_p must be allowed for and thus D_p can be specified mathematically. Some reasons for decreased mass transport at high protein concentration can be considered as follows.

High protein concentrations result in an increase of the viscosity. However, this effect would be by far insufficient for explaining the difference of magnitude almost one order. Some authors examined the influence of electrostatic interactions of proteins among themselves on the diffusion coefficient. Experiments with BSA (18) and lysozyme (19) however demonstrate that above an ionic strength of 0.2 *M* NaCl, a concentration dependency of the free diffusion coefficient cannot be established. Therefore, the investigations with rh-bFGF at 0.5 *M* NaCl are probably within a range, within which such an influence constitutes only a small proportion. In pulsed field gradient NMR studies, a

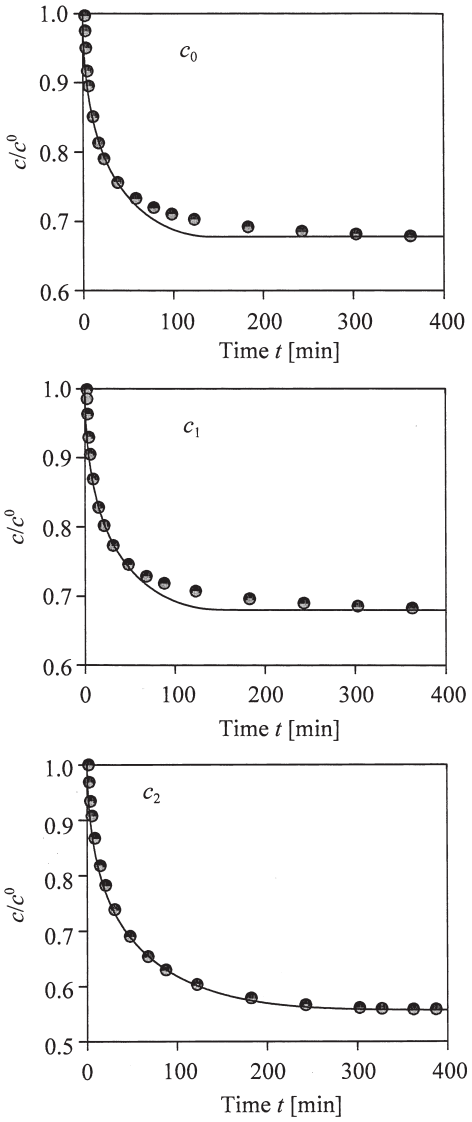

Figure 2. Film and pore diffusion model: modeling (solid lines) and experimental data (●) from uptake curves of rh-bFGF on Heparin HyperD at different initial concentrations, as stated in Table 1, in 50 m*M* sodium phosphate + 0.5 *M* NaCl + 1 m*M* EDTA, pH 6.3, $\kappa = 46.9\,\mathrm{mS\,cm^{-1}}$.

Table 1. Mass Transfer Coefficient as Function of the Recombinant Human Basic Fibroblast Growth Factor (rh-bFGF) Concentration During Adsorption on Heparin HyperD

	c_0	c_1	c_2
c^0 (mg mL^{-1})	2.25	1.18	0.28
D_p (m^2 sec^{-1} $\times$ 10^{-12})	2.5	4.5	9.5
$q^* q_m^{-1}$	0.9	0.75	0.47

concentration dependency of the diffusion coefficient of proteins is well established [see, for example, Ref. (20)]. Nonetheless, the effects being expected are too small to explain the difference in D_p for the concentration range covered. This points out that the assumption of an exclusive mass transport in the pore system by diffusion in the liquid phase is possibly invalid and must be supplemented by another mechanism.

Another explanation for the concentration dependency of D_p is the acceptance of an additional mass transport mechanism, such as a protein diffusion along the surface of the sorbent. This interpretation was applied to different protein systems (21,22) and it was also considered for smaller molecules (23,24); the effect is usually best seen with sorbents of high binding capacity. A direct proof that surface diffusion of proteins may indeed in some cases take place was only given recently, using confocal scanning laser microscopy (25,26). Yet, the occurrence of higher D_p values than those of the free diffusivity strongly support mass transport by surface diffusion. In the case of rh-bFGF adsorption on Heparin HyperD, the D_p was always lower than D_b. Although this result does not indicate the absence of a protein surface diffusion, it does neither strongly support it. With the observed D_p values, tortuosity factors [see Eq. (3)] are calculated within the range of $\tau = 6-22$, which can be regarded as physically meaningful in the context of the pore diffusion model.

Furthermore, against surface diffusion it can be argued that the interactions between Heparin and rh-bFGF are commonly considered as affinity interactions, involving specific interaction sites of both molecules (17). Owing to multiple interactions at those sites, the proportion of surface diffusion to the mass transport is usually considered negligible (27). However, this argument is only tenable, if the electrostatic interactions responsible for the binding are indeed selective for the target protein. For rh-bFGF, this seems to be the case as it can be applied at 0.5 *M* NaCl concentration, which is rather high compared to a typical ion exchanger. On the basis of the measured Langmuir parameters, a classification of the interaction type remains open; common values on ion exchangers would also fall in the observed range.

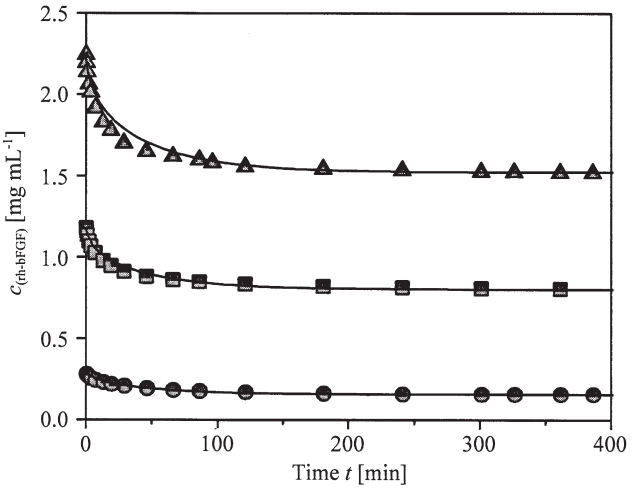

Figure 3. Homogeneous diffusion model: modeling (solid lines with $D_h = 4.0 \times 10^{-14}\,m^2\,sec^{-1}$) and experimental data of rh-bFGF uptake by Heparin HyperD in batch experiments at different initial concentrations in 50 m*M* sodium phosphate + 0.5 *M* NaCl + 1 m*M* EDTA, pH 6.3, $\kappa = 46.9$ mS; (●) $c^0 = 2.25\,mg\,mL^{-1}$, (■) $c^0 = 1.18\,mg\,mL^{-1}$, (▲) $c^0 = 0.28\,mg\,mL^{-1}$.

In Fig. 3, the curves calculated with the homogeneous diffusion model are presented. It is found that the experimental data can be modeled very well with a constant diffusion coefficient of $D_h = 4.0 \times 10^{-14}\,m^2\,sec^{-1}$, i.e., independent of the protein concentration. Compared to D_p, D_h is about 100-times lower, as was to be expected owing to the larger concentration gradients in the stationary phase ($\partial q/\partial r$)—the driving force—in the homogeneous diffusion approach than with the pore diffusion in the pore fluid ($\partial c_p/\partial r$). In addition, with the adsorption of lysozyme to different ion exchangers similar values for D_h were found within a range of 10^{-14}–$10^{-13}\,m^2\,sec^{-1}$ (22).

From these results, it is to be concluded from both model approaches that surface diffusion of proteins on Heparin HyperD contributes to the mass transfer in the porous system.

Isocratic Elution

For the modeling of isocratic column experiments, thermodynamic (adsorption isotherm) and kinetic data (mass transfer by diffusion) from uptake curves were employed. Figure 4 shows the experimentally determined isocratic

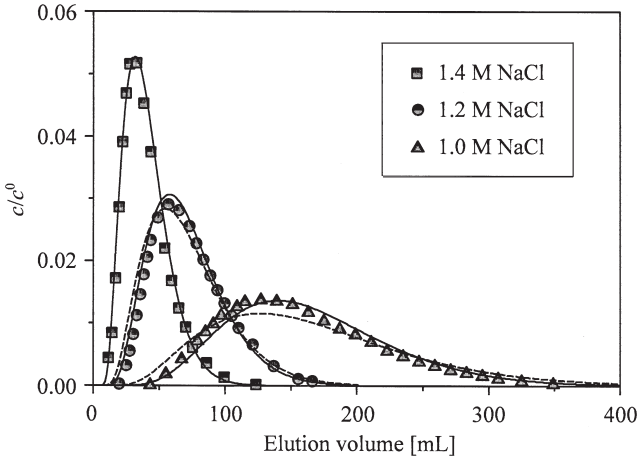

Figure 4. Modeling of isocratic elution of rh-bFGF with the FPD model at different salt concentrations; $c^0 = 1.37\,\text{mg mL}^{-1}$, $V_{\text{inj}} = 2\,\text{mL}$, 50 m*M* sodium phosphate + 1 m*M* EDTA, pH 6.3, $u_0 = 306\,\text{cm hr}^{-1}$; (- - -) $D_p = 2.25 \times 10^{-11}\,\text{m}^2\,\text{sec}^{-1}$, (—) D_p adjusted for optimal fit.

elution profiles of rh-bFGF at salt contents between 1.0 and 1.4 *M* NaCl. Lower concentrations than 1.0 *M* NaCl would lead to still broader peaks and very large elution volumes due to strongly increasing interactions. Broken lines display calculated elution profiles from the FPD model by using the diffusion coefficient determined for 1.4 *M* NaCl. Obviously, this does not yield an optimal fitting at the lower salt concentrations; adjusted values are shown by the solid lines. Peak form and position can be described with the model, whereby for correct peak positioning, minor modifications of the isotherm parameters q_m and K_D were necessary; the values employed in the modeling are indicated in Fig. 1. Pore diffusion coefficients resulting from these experiments are compiled in Table 2. They are within a range of $2.25–3.52 \times 10^{-11}\,\text{m}^2\,\text{sec}^{-1}$, which is clearly much higher than in the batch investigations. Considering the fact that the free protein concentration in the pores is much lower in isocratic elution than in batch adsorption, here the trend of a concentration dependency of D_p is continued. By assigning the best fit D_p to the applied protein concentration (c^0) in batch uptake curves and to the measured protein concentration at peak maximum in isocratic elution experiments (see Fig. 4), which is a rough estimate, an apparent exponential decay of D_p with the protein concentration is observed (Fig. 5). At higher salt concentration also a higher concentration of rh-bFGF is found in the pores, consequently yielding a reverse order of salt concentration and D_p. Apart from the need to adjust the D_p-values, possibly as a result of a surface diffusion

Table 2. Model Parameters Used to Calculate the Isocratic Elution Profiles with the Film and Pore Diffusion Model as Shown in Fig. 4

	1.4 *M*	1.2 *M*	1.0 *M*
D_p ($m^2\,sec^{-1} \times 10^{-11}$)	2.25	2.8	3.52
Sh	20.6	20.6	20.6
Bi	65.2	52.4	41.6
q_m ($mg\,mL^{-1}$)	20	27	41
K_D ($mg\,mL^{-1}$)	4.8	3.3	2

that is not taken care of, the difference could also be related to different fluid dynamics in the column compared with the stirred tank reactor. This aspect is discussed in more detail with the homogeneous diffusion model. All D_p-values used during parameter fitting are below $D_b = 9.3 \times 10^{-11}\,m^2\,sec^{-1}$. Thus tortuosity factors, τ, are calculated between 2.4 and 1.6, which are physically in good agreement with the usual assumptions of pore diffusion.

Isocratic elution experiments carried out with a salt concentration of 1.4 *M* NaCl and linear flow rates between 153 and 458 $cm\,hr^{-1}$ demonstrated that the pore diffusion coefficient, as determined with $2.25 \times 10^{-11}\,m^2\,sec^{-1}$ at 306 $cm\,hr^{-1}$ could be maintained (Fig. 6). Very good predictions were thus

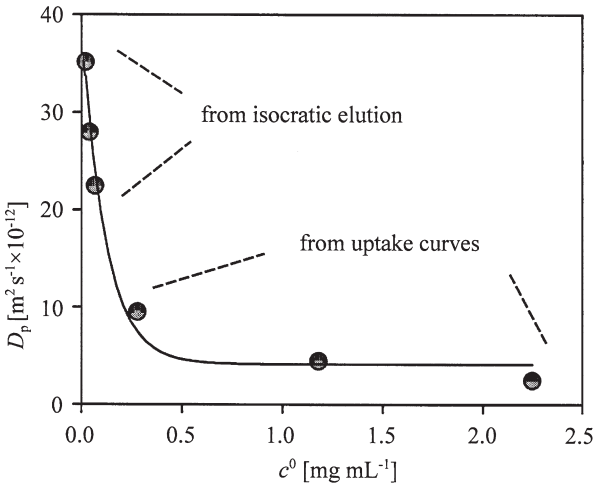

Figure 5. Course of D_p in dependence of protein concentration, as determined directly from batch uptake curves (c^0) and as estimated from isocratic elution by assigning it to the concentration at peak maximum.

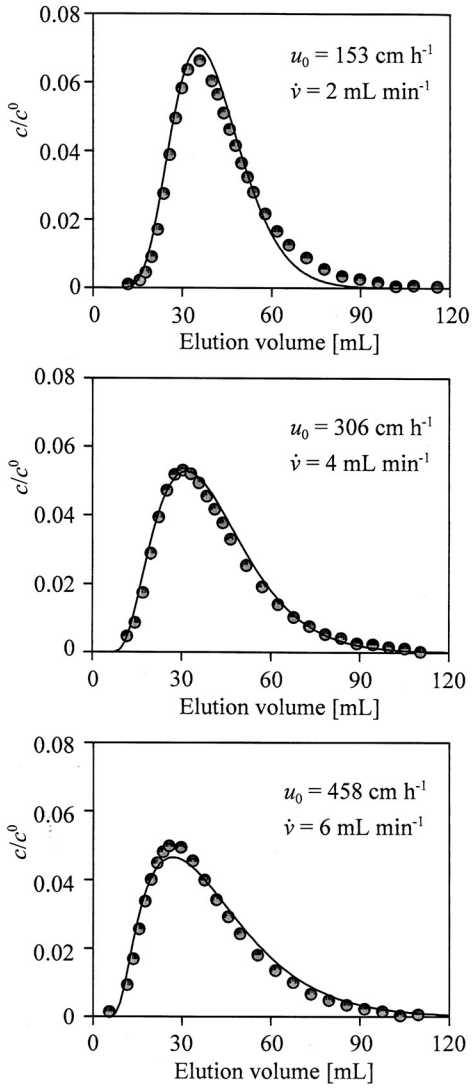

Figure 6. Film and pore diffusion model: modeling of isocratic elution profiles (—) and experimental data (●) at different flow rates; $c^0 = 1.37\,\text{mg mL}^{-1}$, $V_{\text{inj}} = 2\,\text{mL}$, 50 m*M* sodium phosphate + 1.4 *M* NaCl + 1 m*M* EDTA, pH 6.3.

achieved for different flow rates. Therefore, from these experiments no indication is derived that the assumptions regarding the axial dispersion and the hydrodynamics in the packed bed are not justified.

Isocratic elution can also be described with the homogeneous diffusion model, as shown in Fig. 7 for different flow rates. Here the best fit was obtained with a diffusion coefficient of $D_h = 3 \times 10^{-12}\,m^2\,sec^{-1}$. Compared with $D_h = 4.0 \times 10^{-14}\,m^2\,sec^{-1}$ from uptake curves, this value is roughly 2 orders of magnitude higher. Assuming that D_h is independent from the protein concentration, as was found in batch experiments, this result may be explained by the distinct fluid dynamics in the packed bed and the stirred tank experiments. Assuming a pore structure with large continuous pores in the stationary phase, an additional convective mass transport through the particle could be taken into consideration. By such an intra-particulate flow, the diffusion distances to binding sites in the particle center would be shortened, which would be expressed by an increased diffusion coefficient in the modeling. Using the FPD model however does not demonstrate a tendency of increasing D_p with the flow rate (Fig. 6); consequently, the assumption that perfusion is taking place is not supported with this model. On the other hand, the high value of $D_h = 3.0 \times 10^{-12}\,m^2\,sec^{-1}$ cannot be explained by sole surface diffusion. Speaking in the order of magnitudes, it is clearly near the pore diffusion coefficients for proteins. After all, from these measurements no decision can be drawn about the processes involved in the mass transport of rh-bFGF into the particle interior.

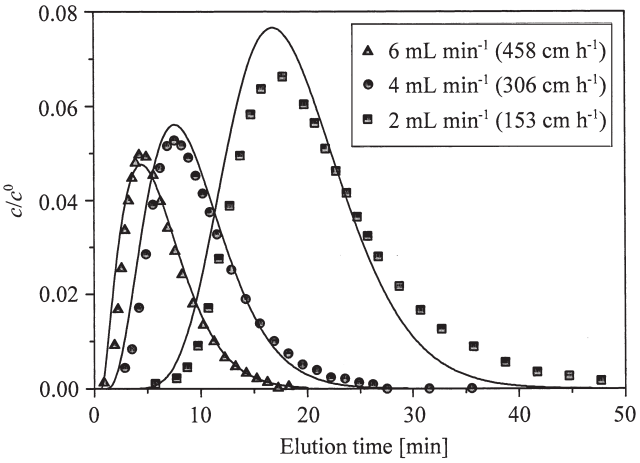

Figure 7. Homogeneous diffusion model: modeling of isocratic elution profiles (—) and experimental data points at different flow rates; $c^0 = 1.37\,mg\,mL^{-1}$, $V_{inj} = 2\,mL$, 50 m*M* sodium phosphate + 1.4 *M* NaCl + 1 m*M* EDTA, pH 6.3.

Gradient Elution

The last step for the application of the models to a real chromatographic system is their application in gradient elution. Figure 8 shows a chromatogram from the downstream process of rh-bFGF described previously (11). Substances in the breakthrough during sample application mainly correspond to remaining DNA, not to rh-bFGF. The rh-bFGF monomer elutes at a salt concentration between 0.9 and 1.2 *M* NaCl in the gradient and can be separated from the rh-bFGF dimer, eluting at about 2 *M* NaCl.

It was found that the experimental data is best fitted with a D_p value of $7 \times 10^{-12}\,m^2\,sec^{-1}$, which is between the D_p-values derived from batch adsorption and isocratic elution. Lower and higher D_p-values are less suitable and lead to more or less marked deviations from the experiment. This indicates that the mass transport is indeed limited by pore and not film diffusion. In gradient elution, very low protein concentrations are realized during loading and high concentrations at the peak maximum. A comparison of experiment and simulation demonstrates that the elution time in the gradient is well described, i.e., the implementation of the adsorption isotherms using the simple linear dependency of q_m and exponential dependency of K_D as function of the salt concentration is justified. In addition, the transfer of the data from simple batch to

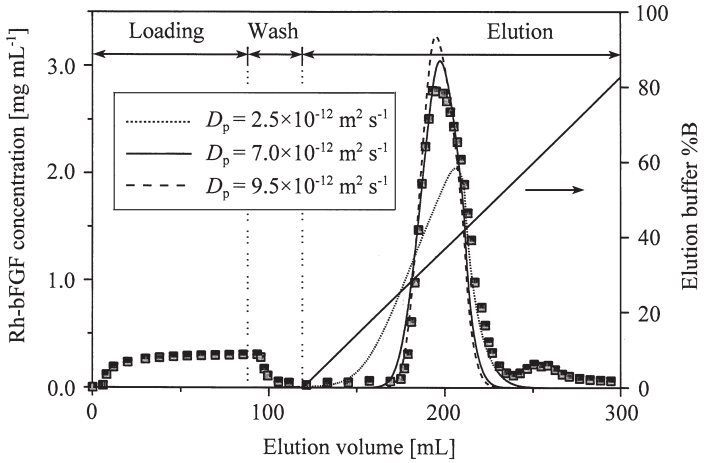

Figure 8. Film and pore diffusion model: modeling (lines corresponding to different D_p) and experimental data from UV measurements at 280 nm (■) of the gradient elution profile during rh-bFGF purification; adsorption with $c^0 = 2.37\,mg\,mL^{-1}$, $V_{inj} = 90\,mL$, 50 m*M* sodium phosphate + 0.5 *M* NaCl + 1 m*M* EDTA, pH 6.3; elution with buffer B: 50 m*M* sodium phosphate + 3.0 *M* NaCl + 1 m*M* EDTA, pH 6.3.

column experiments is possible without problems. Regarding the peak form it is noticed that the peak front is described satisfactorily whereas the tailing of the peak is descending too steeply in the simulation. Here the reason is most probably related to weak additional interactions at high ionic strengths, which are neglected in the model (zero interaction sites are assumed above 1.6 *M* NaCl from Fig. 1). This deviation could be improved probably by considering these interactions also in the model; however it is questioned, whether this is practically relevant.

Regarding the situation at higher flow rates (Fig. 9), it is to be considered that the calculated chromatograms display a fronting compared to the experimental data. At these higher flow rates the same D_p value of $7.0 \times 10^{-12}\,m^2\,sec^{-1}$ was employed as determined at $153\,cm\,hr^{-1}$. This means that at higher flow rates the mass transfer into the particles is faster than expected from the FPD model. Since the film limitation is not to be considered at a flow rate of $153\,cm\,hr^{-1}$, this result is a further indication for a change in fluid dynamics, i.e., this also points towards convective flow in the particle. As this is contradictive to the results obtained from isocratic elution at different flow velocities, this again points out how sensitive the employed models are by changing chromatographic modi.

An investigation of the gradient elution using the homogeneous diffusion model is pending owing to difficulties of the mathematical conversion of the salt dependency of the parameters at the particle edge.

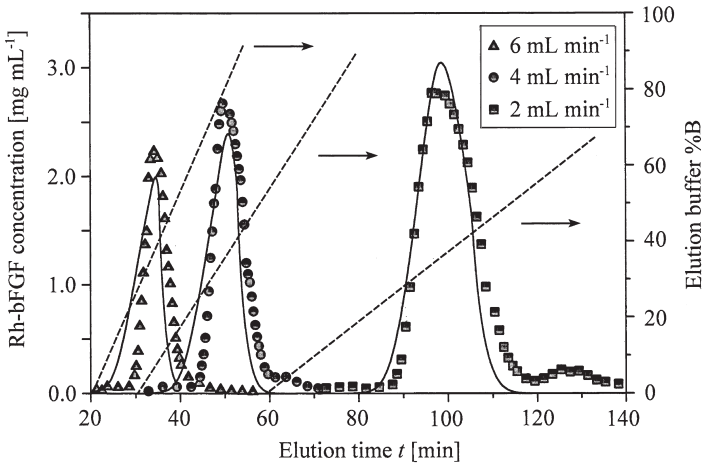

Figure 9. Film and pore diffusion model: modeling (solid lines) and experimental data points of the gradient elution profiles at different flow rates. Experimental conditions as in Fig. 8 with $D_p = 7.0 \times 10^{-12}\,m^2\,sec^{-1}$.

Character of Hyperdiffusion

The name HyperD (hyperdiffusion), for which more frequently the term "enhanced diffusion" is used in literature, implies a mass transport due to diffusion in a fluid. However, the fast diffusion observed is probably linked to a homogeneous or surface diffusion process instead, as discussed in several publications using different proteins (28–30). Others suggested a convective mass transport being responsible for this effect (31,32). Using the ion exchanger Q HyperD with 35 μm particle size, which should display a similar pore structure as the present support, perfusion was found to begin at a linear flow rate of about 150 cm hr^{-1}; at lower flow rates pore diffusion prevails. As arguments for perfusive flow in pores, a constant theoretical plate height and increasing diffusion coefficients over the flow rate are mentioned. Since the Heparin HyperD sorbent used here is of twice the particle size, perfusion should begin at a higher linear flow rate. For deriving appropriate conclusions about the real mass transfer mechanism of rh-bFGF inside the pore structure of Heparin HyperD, further investigations are necessary. In this respect, it must be addressed whether or not surface diffusion is indeed taking place as well as the different fluid dynamics in the stirred tank and the packed bed. To follow the mass transfer in view of a surface diffusion process, a method is required, which traces the migration of proteins to the interior of an adsorbent particle. A promising starting point in this direction represents confocal scanning laser microscopy (33), which can follow the migration of a protein labeled with a fluorophore into the interior of an adsorbent fixed by a laser beam. Thus, the proceeding protein concentration in a particle can be resolved in time intervals. Recently, an attempt was made to distinguish between pore and surface diffusion by consequent adsorption of two differently labeled proteins. From these investigations, it was concluded that different proteins may show different mechanisms of intra-particulate transport. Although the interpretation given is plausible, still a direct distinction between pore and surface diffusion remains to be shown; especially, the existence of surface diffusion is to be established.

For practical use, gradient elution is mathematically well described using the FPD model, considering the empirically determined dependence of adsorption isotherms from the salt concentration. Different flow rates can be well implemented using an average diffusion coefficient. In view of a more exact process interpretation the isotherm parameters of the side products and/or the dimer of rh-bFGF would have to be considered. Then a process could be designed, e.g., regarding the separation power between these components by using different flow rates or gradient forms.

CONCLUSIONS

Batch adsorption of rh-bFGF on the affinity sorbent Heparin HyperD as well as isocratic elution can be described with both the FPD model and the homogeneous diffusion model. Affinity purification of rh-bFGF from a mixture containing remaining amounts of DNA and host-specific proteins by gradient elution could be described with the FPD model. Modeling of gradient elution with the homogeneous diffusion model could not be shown owing to problems caused by the mathematical implementation; yet, it was not indicated that this is a general problem and therefore results from isocratic elution should be applicable also to gradient elution.

Both models, however, showed weak points also. The concentration dependency of the pore diffusion coefficient in the FPD model indicates that the assumption of a sole diffusive mass transport in the pore fluid of the sorbent is not tenable. Another problem is linked to the structure of the sorbent, which might allow convective flow to occur through the particle. If this is true, it would explain the necessary increases of D_p and D_h by applying them from batch uptake curves to packed bed experiments. These problems prevent an unrestricted usage of a mathematical model and do not allow it to be recommended as a user-friendly tool. It also demonstrates that fundamentals of protein adsorption inside a porous sorbent are not solved completely, especially the contributing driving forces and mass transport limitations.

The latter points out that analytical methods are required still, which allow to trace the protein during its migration through the porous system of an adsorbent. A promising method might be confocal scanning laser microscopy, which has demonstrated that a general differentiation of the protein transport by pore or surface diffusion does not take into account the complexity of these molecules.

Until the distinct adsorption behavior of different proteins on the various chromatographic sorbents is not unraveled and therefore cannot be generalized, adapting mathematical models of chromatographic elution remains necessary for each single case.

NOMENCLATURE

Bi	Biot number $= k_f R_p \varepsilon_p^{-1} D_p^{-1}$
C^0	start concentration at time $t = 0$ (mg mL^{-1})
$c_{0,i}(t)$	concentration at column inlet (mg mL^{-1})
c_b	bulk (void) volume concentration (mg mL^{-1})
c_p	pore volume concentration (mg mL^{-1})
D_{ax}	axial dispersion coefficient (m^2 sec^{-1})
D_b	bulk diffusion coefficient (m^2 sec^{-1})

D_h	homogeneous diffusion coefficient ($m^2\,sec^{-1}$)
d_p	particle diameter (m)
D_p	pore diffusion coefficient ($m^2\,sec^{-1}$)
K_D	dissociation constant $K_D = k_d/k_a$ (Langmuir) ($mg\,mL^{-1}$)
k_f	film mass-transfer coefficient ($m\,sec^{-1}$)
L	column length (bed dimension) (m)
q	concentration of adsorbed protein ($mg\,mL^{-1}$)
q^*	concentration of adsorbed protein at equilibrium ($mg\,mL^{-1}$)
q_m	maximal saturation capacity (Langmuir) ($mg\,mL^{-1}$)
r	particle coordinate (diameter, from 0 to R_p) (m)
Re_0	Reynolds number $= \rho_l d_p u_0 \eta$
R_p	particle radius (m)
Sc	Schmidt number $= \eta \rho_l^{-1} D_b^{-1}$
Sh	Sherwood number $= 2 r_p k_f D_b^{-1}$
t	time (sec)
u_0	interfacial fluid velocity ($m\,sec^{-1}$)
u_i	interstitial fluid velocity ($m\,sec^{-1}$)
z	column coordinate in axial direction (from 0 to L) (m)

Greek Symbols

η	fluid viscosity (Pa sec)
ρ_l	fluid density ($mg\,mL^{-1}$)
τ	tortuosity factor
ε_b	void volume fraction
ε_p	pore volume fraction of stationary phase

Subscripts

*	equilibrium situation (adsorption)
b	bulk
i	index of components
p	pore

ACKNOWLEDGMENTS

We thank A. Walter for the technical assistance.

REFERENCES

1. Ramsden, J.J. Puzzles and Paradoxes in Protein Adsorption. Chem. Soc. Rev. **1995**, *24* (1), 73–78.

2. Ruthven, D.M. *Principles of Adsorption and Adsorption Processes*; Wiley: New York, 1984.
3. Arve, B.H.; Liapis, A.I. The Modeling and Analysis of the Elution Stage of Biospecific Adsorption in Fixed Beds. Biotechnol. Bioeng. **1987**, *30*, 638–649.
4. Gu, T.; Tsai, G.-J.; Tsao, G.T. New Approach to a General Nonlinear Multicomponent Chromatography Model. AIChE J. **1990**, *36*, 784–788.
5. Berninger, J.A.; Whitley, R.D.; Zhang, X.; Wang, N.H. A Versatile Model for Simulation of Reaction and Nonequilibrium Dynamics in Multicomponent Fixed-Bed Adsorption Processes. Computers. Chem. Eng. **1991**, *15*, 749–768.
6. Gallant, S.R.; Vunnum, S.; Cramer, S.M. Modeling Gradient Elution of Proteins in Ion-Exchange Chromatography. AIChE J. **1996**, *42*, 2511–2520.
7. Luo, R.; Hsu, J.T. Rate Parameters and Gradient Correlations for Gradient-Elution Chromatography. AIChE J. **1997**, *43*, 464–474.
8. Gallant, S.; Kundu, A.; Cramer, S.M. Modeling Non Linear Elution of Proteins in Ion-Exchange Chromatography. J. Chromatogr. A **1995**, *702*, 125–142.
9. Burgess, W.H.; Maciag, T. The Heparin-Binding Growth Factor Family of Proteins. Ann. Rev. Biochem. **1989**, *58*, 575–606.
10. Seeger, A.; Schneppe, B.; McCarthy, J.E.G.; Deckwer, W.-D.; Rinas, U. Comparison of Temperature- and Isopropyl-β-D-thiogalacto-pyranoside-Induced Synthesis of Basic Fibroblast Growth Factor in High-Cell-Density Cultures of Recombinant. Enzyme Microb. Technol. **1995**, *17*, 947–953.
11. Garke, G.; Deckwer, W.-D.; Anspach, F.B. Preparative Two Step Purification of Recombinant Human Basic Fibroblast Growth Factor From High Cell Density Cultivation of *E. coli*. J. Chromatogr. B **2000**, *737*, 25–38.
12. Geankoplis, C.J. *Transport Processes and Unit Operations*, 2nd Ed.; Allyn and Bacon Inc.: Massachusetts, 1983.
13. Garke, G. *Mathematische Simulation Chromatographischer Prozesse am Beispiel der Aufarbeitung von rh-bFGF aus der* E. coli *Hochzelldichtefermentation sowie von Modellproteinen*; Fortschr.-Ber. VDI Reihe 17 Nr. 199, VDI-Verlag: Düsseldorf, 2000.
14. Chung, S.F.; Wen, C. Longitudinal Dispersion of Liquid Flowing Through Fixed and Fluidized Beds. AIChE J. **1968**, *14* (6), 857–866.
15. Wilson, E.J.; Geankoplis, C.J. Liquid Mass Transfer at Very Low Reynolds Numbers in Packed Beds. I EC Fundam. **1966**, *5* (1), 9–14.
16. NAG, Numerical Algorithms Group Ltd., 1400 Opus Place, Suite 200, Downers Grove, IL 60515.

17. Zhang, J.; Cousens, L.S.; Barr, P.J.; Sprang, S.R. Three-Dimensional Structure of Human Basic Fibroblast Growth Factor, a Structural Homolog of Interleukin 1β. Proc. Natl Acad. Sci. USA **1991**, *88*, 3446–3450.
18. Raj, T.; Flygare, W.H. Diffusion Studies of Bovine Serum Albumin by Quasielastic Light Scattering. Biochemistry **1974**, *13*, 3336–3340.
19. Nyström, B.; Johnsen, R.M. Effect of Concentration and Ionic Strength on the Translational Diffusion Coefficient of Lysozyme. Chemica Scripta **1983**, *22*, 82–84.
20. Pan, H.; Barany, G.; Woodward, C. Reduced BPTI Is Collapsed. A Pulsed Field Gradient NMR Study of Unfolded and Partially Folded Bovine Pancreatic Trypsin Inhibitor. Protein Sci. **1997**, *6*, 1985–1992.
21. Yoshida, H.; Yoshikawa, M.; Kataoka, T. Parallel Transport of BSA by Surface and Pore Diffusion in Strongly Basic Chitosan. AIChE J. **1994**, *40*, 2034–2044.
22. Chang, C.; Lenhoff, A.M. Comparison of Protein Adsorption Isotherms and Uptake Rates in Preparative Cation-Exchange Materials. J. Chromatogr. A **1998**, *827*, 281–293.
23. Yang, S.A.; Pyle, D.L. The Adsorption Kinetics of Cephalosporin-c on Nonionic Polymeric Macropore Amberlite XAD-16 Resin. J. Chem. Technol. Biotechnol. **1999**, *74*, 216–220.
24. Al-Duri, B.; McKay, G. Pore Diffusion: Dependence of the Effective Diffusivity on the Initial Sorbate Concentration in Single and Multisolute Batch Adsorption Systems. J. Chem. Technol. Biotechnol. **1992**, *55*, 245–250.
25. Thömmes, J.; Linden, T.; Ljunglöf, A. Visualizing Protein Transport in Porous Adsorbents by Confocal Microscopy. Biotechnology 2000, 11th International Biotechnology Symposium and Exhibition, Berlin, Germany, Book of Abstracts, 2000; 445.
26. Linden, T.; Ljunglöf, A.; Halfar, M.; Thömmes, J. Investigation of Internal Protein Transport into Porous Adsorbents by Confocal Laser Scanning Microscopy CLSM. SPICA 2000, International Symposium on Preparative and Industrial Chromatography and Allied Techniques, Zürich, Switzerland, Book of Abstracts, 2000; 128.
27. Liapis, A.I. Theoretical Aspects of Affinity Chromatography. J. Biotechnol. **1989**, *11*, 143–160.
28. Boschetti, E.; Coffman, J.L. Enhanced Diffusion Chromatography and Related Sorbents for Biopurification. In *Bioseparation and Bioprocessing*; Subramanian, G. Ed.; Wiley-VCH: Weinheim, 1998, 157–198.
29. Horvath, J.; Boschetti, E.; Guerrier, L.; Cooke, N. High-Performance Protein Separations with Novel Strong Ion Exchangers. J. Chromatogr. A **1994**, *679*, 11–22.

30. Wright, P.R.; Muzzio, F.J.; Glasser, B.J. Batch Uptake of Lysozyme: Effect of Solution Viscosity and Mass Transfer on Adsorption. Biotechnol. Prog. **1998**, *14*, 913–921.
31. Rodriguez, A.E. Permeable Packings and Perfusion Chromatography in Protein Separation. J. Chromatogr. B **1997**, *699*, 47–61.
32. Rendueles de la Vega, M.; Chenou, C.; Loureiro, J.M.; Rodrigues, A.E. Mass Transfer Mechanism in HyperD Media for Chromatographic Protein Separation. Biochem. Eng. J. **1998**, *1*, 11–23.
33. Ljunglöf, A.; Thömmes, J. Visualising Intraparticle Protein Transport in Porous Adsorbents by Confocal Microscopy. J. Chromatogr., A **1998**, *813*, 387–395.